Supplementary Materials and methods for abamine synthesis

General information

All starting materials were used as received from commercial sources without further purification. All reactions were performed in round-bottom flasks fitted with rubber septa using the standard laboratory techniques. Reactions sensitive to air and/or moisture were performed under a positive pressure of argon. Analytical thin-layer chromatography (TLC) was performed using aluminum plates pre-coated with silica gel (silica gel 60 F254). TLC plates were visualized by exposure to ultraviolet light and then were stained by submersion in basic potassium permanganate solution or in ethanolic phosphomolybdic acid solution followed by brief heating. Column chromatography was performed on silica gel 60 (40-63 μm). Melting points (mp) were tested on a capillary melting point apparatus. ^{1}H NMR and ^{13}C NMR spectra were recorded on 500 and 125 MHz in $CDCl_3$; chemical shifts (δ ppm) and coupling constants (Hz) of ^{1}H NMR are reported in a standard fashion with relative to the remaining $CHCl_3$ present in $CDCl_3$ (δH = 7.27 ppm). ^{13}C NMR chemical shifts (δ ppm) are reported relative to $CHCl_3$ (δC = 77.23 ppm, central line of triplet). Proton coupling patterns are represented as singlet (s), doublet (d), doublet of doublet (dd), triplet (t), triplet of triplet (tt) and multiplet (m). HRMS data were obtained using quadrupole/ion trap mass analyzer. Analysis and assignments were made by comparison with literature spectroscopic data or using 2D-COSY, HSQC, HMBC, 2D-NOESY and 1D-NOEdiff experiments. The purity of **Aba** was determined by LC-MS (Acquity UPLC™ System, Waters, Milford, MA, USA) consisting of a binary solvent manager and sample manager). Reverse-phased column (Symetry C18, 5μm, 150 mm × 2.1 mm; Waters, Milford, MA, USA). The compound was separated in a linear gradient of MeOH (B) and 15mM ammonium formate adjusted to pH 4.0 (A) at a flow rate of 200 μl/min. Following binary gradient was used: 0 min, 10 % B; 0-24 min. linear gradient to 90 % B; 25-34 min. isocratic elution of 90 % B; 35-45 min. linear gradient to 10 % B. The column was kept at 25 °C. The effluent was introduced then to PDA detector (scanning range 210-700 nm with 1.2 nm resolution) and an electrospray source (source temperature 120 °C, desolvation temperature 300 °C, capillary voltage 3 kV, cone voltage 20 V). Nitrogen was used as well as cone gas (50 l/h) and desolvation gas (500 l/h). Data acquisition was performed in the full scan mode (50-1000 Da), scan time of 0.5 sec. and collision energy of 6 V. Analyses were performed in positive mode (ESI^{+}).

Synthesis overview

Targeted molecule was prepared using modified literature protocol in accessed in 7 steps and 17.5% overall yield (Han et al., 2004).

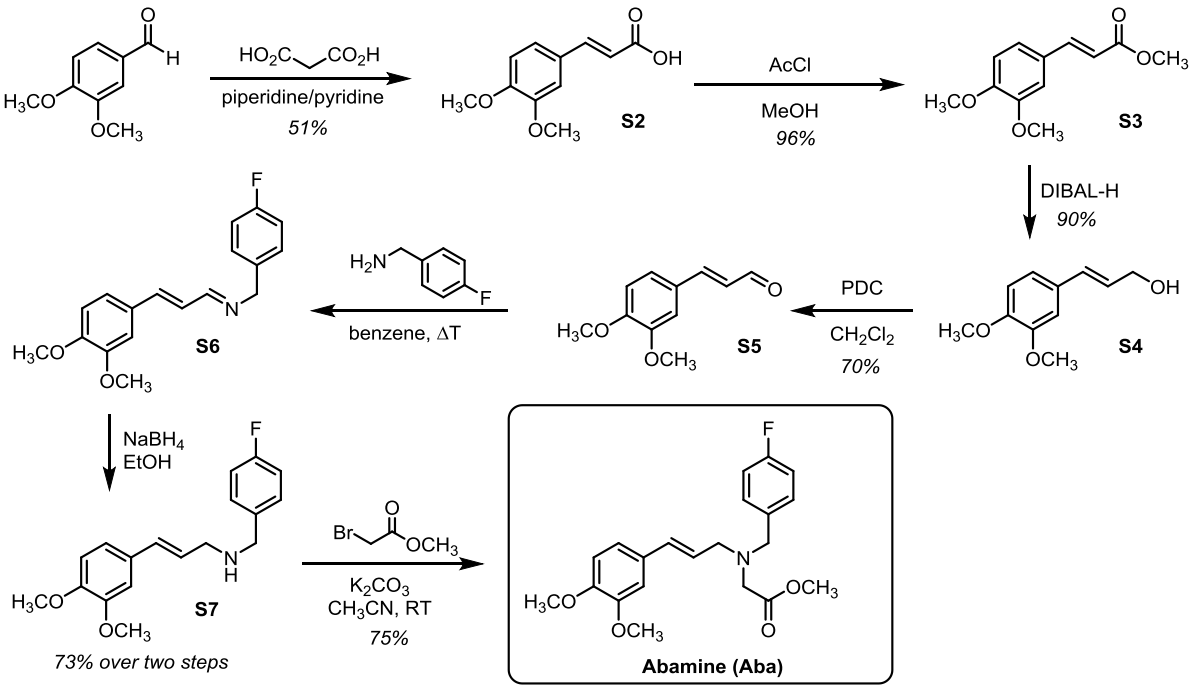

Experimental Protocols

Transformation of aldehyde to methyl ester **S3**

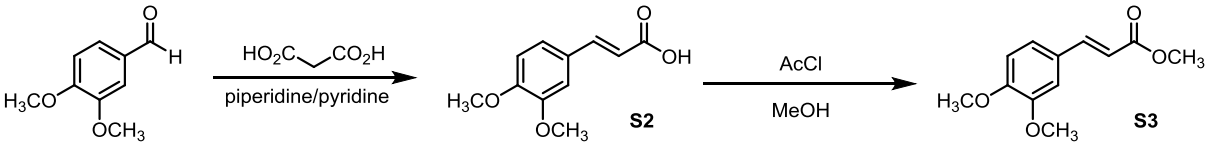

A solution of veratraldehyde (7.0 g, 42.1 mmol, 1.0 equiv) and malonic acid (5.2 g, 63.2 mmol, 1.5 equiv) in pyridine (12 mL, 3.5M to aldehyde) was stirred at RT for 5 min. Piperidine (629 μL, 6.4 mmol, 0.15 equiv) was added and the resulting mixture was stirred at 85°C in Schlenck tube for 8.5h. The resulting mixture was cooled to RT and the Schlenck tube was carefully opened and its contain was poured into ice/water bath (100g/150 mL placed in 500mL beaker). The resulting mixture was vigorously stirred and acid **S2** started to precipitate. When the ice melted, the resulting precipitate was filtered and dried under the vacuum at 30°C yielding acid **S2** (4.49g, 51%) in form of white crystals (m.p. = 178-180°C (from water)); ^{1}H NMR (500 MHz, $CDCl_3$) δ (ppm): 7.75 (d, J = 15.9 Hz, 1H), 7.15 (dd, J = 8.6, 2.0 Hz, 1H), 7.09 (d, J = 2.0 Hz, 1H), 6.89 (d, J = 8.4 Hz, 1H), 6.34 (d, J = 15.9 Hz, 1H), 3.93 (d, J = 0.6 Hz, 6H); ^{13}C NMR (126 MHz, $CDCl_3$) δ (ppm): 172.80, 151.71, 149.44, 147.21, 127.21, 123.37, 115.08, 111.20, 109.92, 56.20, 56.10.

Acid **S2** (4.49g, 21.56 mmol, 1.0 equiv) was dissolved in methanol (21mL, 1.0M) and the whole mixture was cooled to 0°C. Acetyl chloride (1.22 mL, 17.24 mmol, 0.8 equiv) was added and the whole mixture was allowed to warm to RT and stirred at RT for additional 12h. The whole mixture was evaporated under reduced pressure and the residue was purified by column chromatography on silica gel (P.E.:EtOAc = 2:1) yielding the desired ester **S3** as colorless solid (4.6g, 96%). M.p. = 64.5-65.5°C; ^{1}H NMR (500 MHz, $CDCl_3$) δ (ppm): 7.63 (d, J = 16.2 Hz, 1H), 7.10 (dd, J = 8.3, 1.8 Hz, 1H), 7.04 (d, J = 2.1 Hz, 1H), 6.86 (d, J = 8.6 Hz, 1H), 6.31 (d, J = 15.9 Hz, 1H), 3.90 (s, J = 4.6 Hz, 6H), 3.79 (s, 3H); ^{13}C NMR (126 MHz, $CDCl_3$) δ (ppm): 167.84, 151.26, 149.34, 144.96, 127.49, 122.77, 115.61, 111.15, 109.72, 56.12, 56.02, 51.79.

Ester S3 reduction to 3,4-dimethoxycinnamyl alcohol (S4)

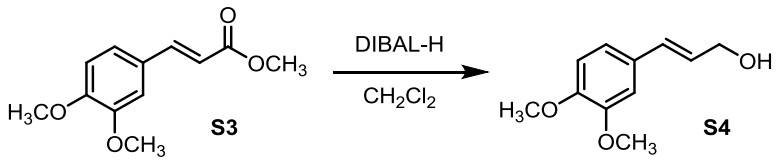

A solution of ester **S3** (3.3g, 13.49mmol, 1.0 equiv) in dry CH_2Cl_2 (27mL, 0.5M) was cooled to 0°C and DIBAL-H (33.7mL, 33.7mmol, 2.5 equiv; 1.0M solution in CH_2Cl_2) was added dropwise. The resulting mixture was stirred at 0°C for 30 min prior the cooling bath removal. After 1h at RT, the reaction mixture was again cooled to 0°C and stirred for 15 min at 0°C. Aqueous saturated solution of Rochel salt (10mL) was added dropwise to quench the reaction and the resulting mixture was stirred at RT for next 13h (milky suspension turned into the clear biphasic solution). Resulting phases were separated and the aqueous layer was extracted with CH_2Cl_2 (3x75mL). Combined organic layers were washed with brine (50mL), dried over Na_2SO_4, filtered and evaporated under reduced pressure. The residue was purified by column chromatography (silica gel; P.E.:EtOAc = 2:1) yielding the desired product **S4** (2.60g, 98%) as colorless solid. M.p. = 76-77°C; ^{1}H NMR (500 MHz, $CDCl_3$) δ (ppm): 6.97 – 6.91 (m, 2H), 6.83 (d, J = 8.3 Hz, 1H), 6.56 (d, J = 15.9 Hz, 1H), 6.26 (dt, J = 15.9, 6.1 Hz, 1H), 4.32 (dd, J = 6.1, 1.5 Hz, 2H), 3.91 (s, 3H), 3.89 (s, 3H); ^{13}C NMR (126 MHz, $CDCl_3$) δ (ppm): 149.20, 149.09, 131.37, 129.89, 126.71, 119.89, 111.25, 108.97, 64.06, 56.10, 56.00.

Transformation of 3,4-dimethoxycinnamyl alcohol S4 to aldehyde S5

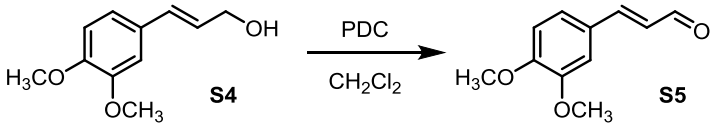

3,4-dimethoxycinnamyl alcohol (**S4**) (1.00 g, 5.1 mmol) in CH_2Cl_2 (10mL) was slowly added via syringe to a mixture of pyridinium dichromate (PDC, 3.86g, 10.3 mmol, 2.0 equiv) in CH_2Cl_2 (20mL). Resulting mixture was stirred for 2 h at RT prior 0.5 mL of methanol was added. The whole mixture was passed through silica gel (filtration) and filter cake was washed with EtOAc (300mL). Organic solvents were removed under reduced pressure and the crude aldehyde was purified by column chromatography (silica gel; P.E.:EtOAc = 4:1) yielding a desired aldehyde **S5** (690mg, 70%) as viscose oil. ^{1}H NMR (500 MHz, $CDCl_3$) δ (ppm): 9.66 (d, J = 7.9 Hz, 1H), 7.42 (d, J = 15.9 Hz, 1H), 7.17 (dd, J = 8.4, 2.0 Hz, 1H), 7.08 (d, J = 2.1 Hz, 1H), 6.91 (d, J = 8.3 Hz, 1H), 6.61 (dd, J = 15.9, 7.6 Hz, 1H), 3.94 (s, 3H), 3.93 (s, 3H); ^{13}C NMR (126 MHz, $CDCl_3$) δ (ppm) 193.78, 153.07, 152.14, 149.54, 127.22, 126.88, 123.64, 111.27, 109.97, 56.22, 56.11; MS (APCI, *m/z*, %): 193 (100) $[M+H]^+$, 210 (26) $[M+NH_4]^+$.

Transformation of 3,4-dimethoxycinnamyl aldehyde S5 to amine S7

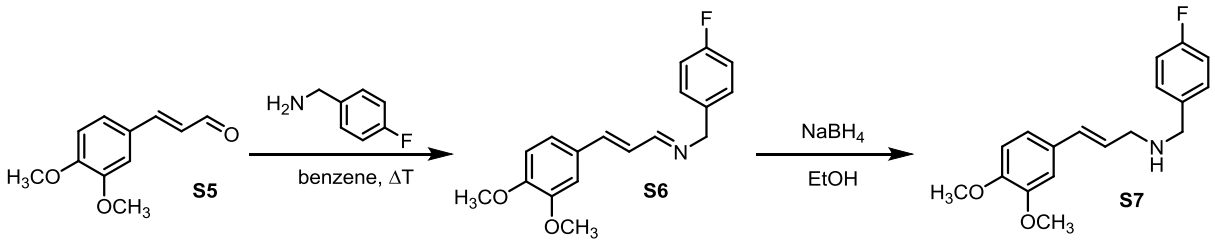

Aldehyde **S5** (690mg, 3.58mmol, 1.0 equiv) was dissolved in benzene (7.2mL, 0.5M) at RT and 4-fluorobenzylamine (429μL, 3.76 mmol, 1.05 equiv) was added. The resulting mixture was stirred at 80°C for 2h. The resulting mixture was evaporated to dryness under vacuum, and the residue, crude imine **S6** was used in the next step.

Imine **S6** (crude material from the previous step) was dissolved in EtOH (12 mL, 0.3M) and the resulting mixture was cooled to 0°C (ice/water). $NaBH_4$ (147mg, 3.89mmol, 1.05equiv) was added portion wise and the resulting mixture was allowed to stir at RT for 2h. The reaction mixture was diluted with water (25mL) and the whole mixture was extracted with CH_2Cl_2 (3x25 mL). Combined organic layers were washed with water (10 mL), brine (10 mL), dried over anhydrous Na_2SO_4, filtered and concentrated under reduced pressure. The crude material was purified by column chromatography (silica gel; CH_2Cl_2:MeOH = 95:5) to give amine **S7** (810mg, 73%) as viscose oil. ^{1}H NMR (500 MHz, $CDCl_3$) δ (ppm): 7.32 (ddd, J = 6.4, 4.9, 2.0 Hz, 2H), 7.05 – 6.98 (m, 2H), 6.95 (d, J = 2.1 Hz, 1H), 6.91 (dd, J = 8.4, 2.0 Hz, 1H), 6.82 (t, J = 7.3 Hz, 1H), 6.48 (d, J = 15.9 Hz, 1H), 6.19 (dt, J = 15.6, 6.6 Hz, 1H), 5.30 (s, 1H), 3.92 (dd, J = 6.1, 2.8 Hz, 2H), 3.90 (s, 3H), 3.88 (s, 3H), 3.44 (dd, J = 12.4, 4.7 Hz, 1H), 3.41 (dd, J = 11.6, 4.0 Hz, 1H); ^{13}C NMR (126 MHz, $CDCl_3$) δ (ppm): 149.20, 148.90, 135.83, 131.72, 130.27, 130.04, 129.98, 126.14, 119.63, 115.51, 115.35, 111.26, 108.77, 56.10, 55.98, 52.65, 51.31.

Alkylation of amine S7 to yield abamine Aba

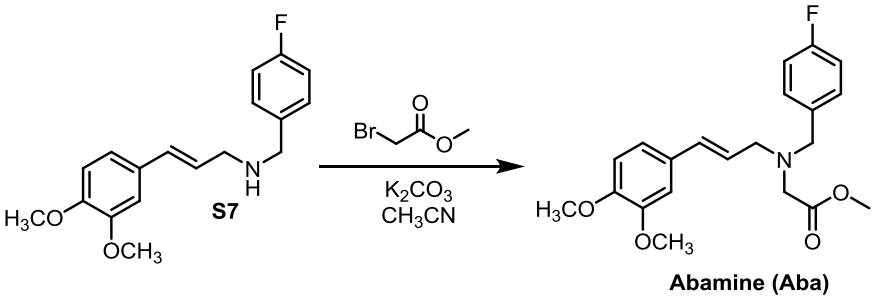

Benzylamine **S7** (810mg, 2.68 mmol, 1.0 equiv) was dissolved in CH_3CN (11 mL, 0.25M) and K_2CO_3 (742mg, 5.37 mmol, 2.0 equiv) was added. After 5 min, methyl bromoacetate (291µL, 3.08 mmol, 1.15 equiv) was added via syringe and the resulting mixture was stirred at RT for 14 h. The reaction mixture was then poured into sat. aq. $NaHCO_3$ (20 mL) and the whole mixture was extracted with CH_2Cl_2 (3x50mL). The combined organic phases were dried over Na_2SO_4, filtered and concentrated under reduced pressure. The resulting crude material was purified by column chromatography (SiO_2; P.E.:EtOAc = 4:1->2:1) yielding the desired abamine **Aba** (749mg, 75%) as colorless viscose oil.

^{1}H NMR (500 MHz, $CDCl_3$) δ (ppm) = 7.35 (dd, J = 8.6, 5.7 Hz, 2H), 7.02 (t, J = 8.7 Hz, 2H), 6.94 (d, J = 2.0 Hz, 1H), 6.90 (dd, J = 8.3, 2.0 Hz, 1H), 6.82 (d, J = 8.3 Hz, 1H), 6.48 (d, J = 15.9 Hz, 1H), 6.11 (dt, J = 15.9, 6.9 Hz, 1H), 3.90 (s, 3H), 3.89 (s, 3H), 3.78 (s, 2H), 3.68 (s, 3H), 3.39 (d, J = 6.1 Hz, 2H), 3.35 (s, 2H); ^{13}C NMR (126 MHz, $CDCl_3$) δ (ppm): 172.04, 149.22, 148.99, 133.07, 130.79, 130.73, 130.14, 125.16, 119.75, 115.41, 115.25, 111.24, 108.78, 57.66, 56.67, 56.13, 56.02, 53.93, 51.65; HRMS (ESI^+; *m/z*): $[M+H]^+$ = 374.74 amu. Elemental analysis: calculated for C21H24FNO4: C = 67.55%; H = 6.48%; N = 3.75; found: C = 67.85%; H = 6.65%; N = 3.48.

LC-MS (Acquity UPLC™ System, Waters, Milford, MA, USA) consisting of a binary solvent manager and sample manager). Reverse-phased column (Symetry C18, 5µm, 150 mm × 2.1 mm; Waters, Milford, MA, USA). The compound was separated in a linear gradient of MeOH (B) and 15mM ammonium formate adjusted to pH 4.0 (A) at a flow rate of 200 µl/min. Following binary gradient was used: 0 min, 10 % B; 0-24 min. linear gradient to 90 % B; 25-34 min. isocratic elution of 90 % B; 35-45 min. linear gradient to 10 % B. The column was kept at 25 °C. The effluent was introduced then to PDA detector (scanning range 210-700 nm with 1.2 nm resolution) and an electrospray source (source temperature 120 °C, desolvation temperature 300 °C, capillary voltage 3 kV, cone voltage 20 V). Nitrogen was used as well as cone gas (50 l/h) and desolvation gas (500 l/h). Data acquisition was performed in the full scan mode (50-1000 Da), scan time of 0.5 sec. and collision energy of 6 V.

Analyses were performed in positive mode (ESI+) therefore data were collected as quasi-molecular ions of [M+H]+. RT (abamine) = 27.90 min, $[M+H]^+$ = 374.74 amu. Purity 98.9%.

Abamine – Copy of ^{1}H and ^{13}C NMR spectra, LC chromatogram, and MS spectra

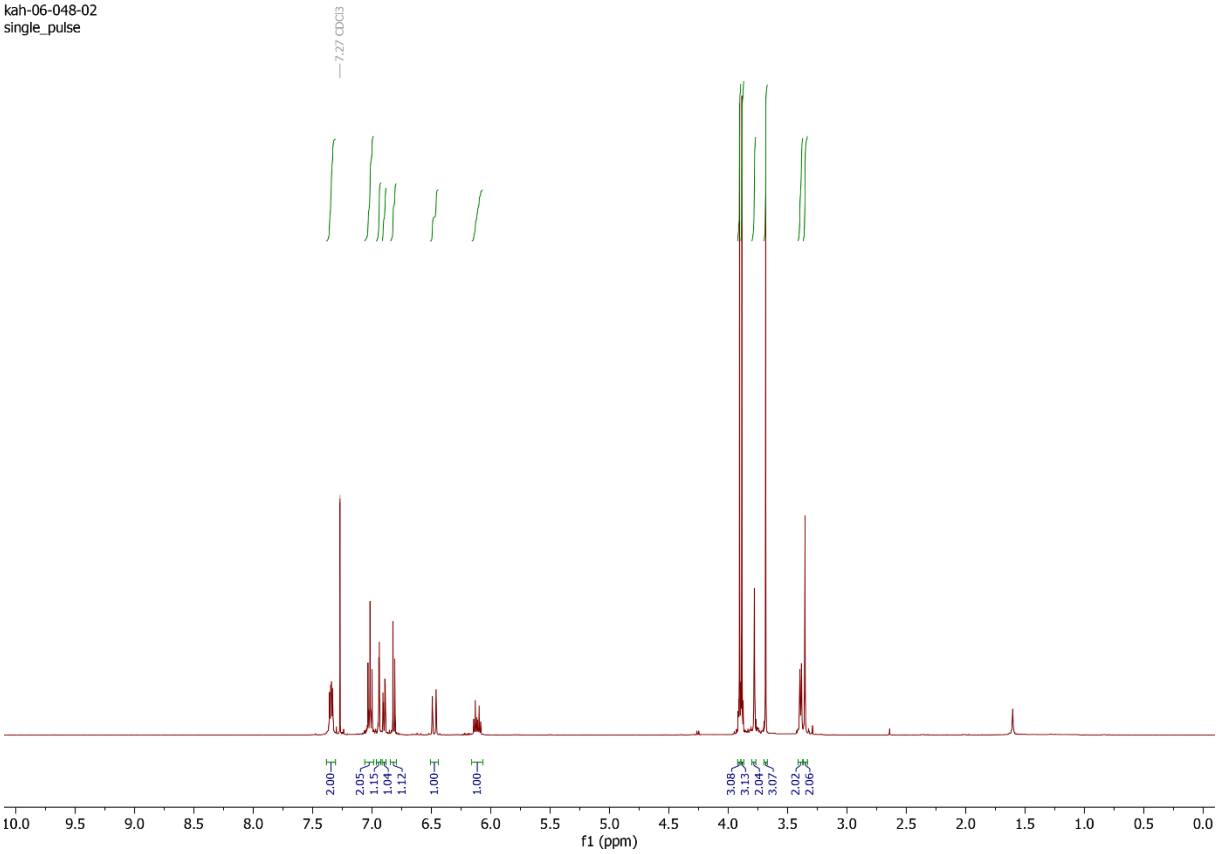

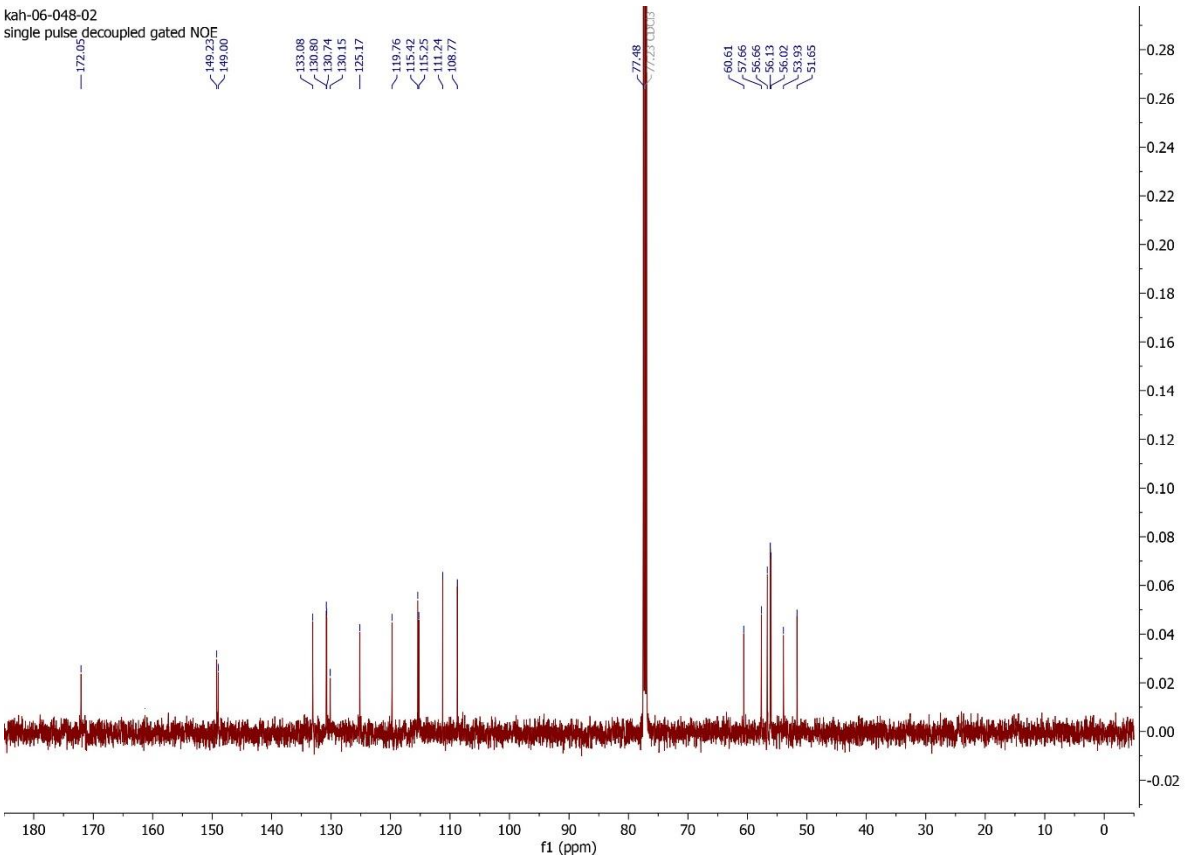

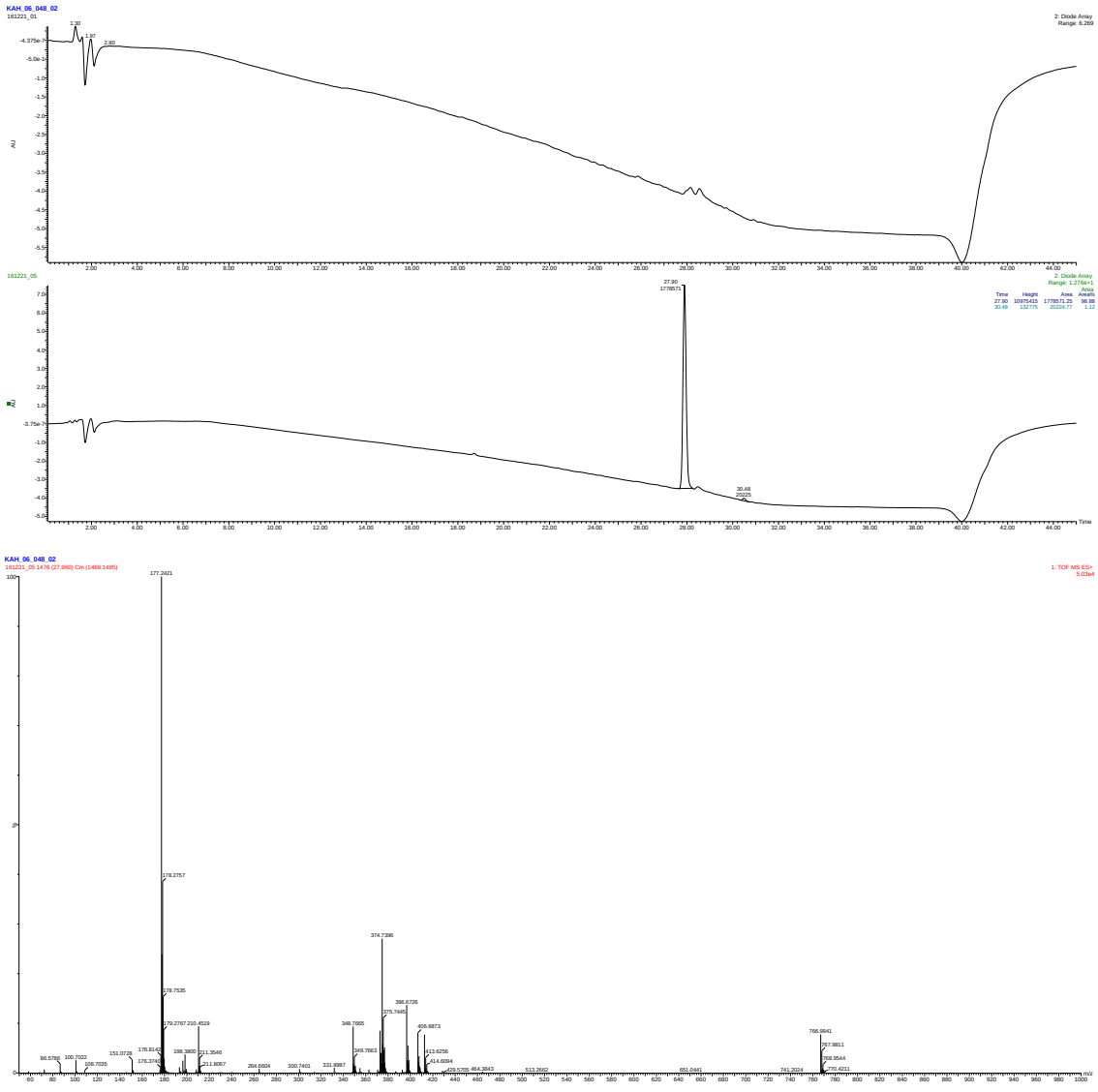

Han, S.-y., Kitahata, N., Saito, T., Kobayashi, M., Shinozaki, K., Yoshida, S., and Asami, T. (2004). A new lead compound for abscisic acid biosynthesis inhibitors targeting 9-cis-epoxycarotenoid dioxygenase. Bioorg. Med. Chem. Lett. **14,** 3033-3036.

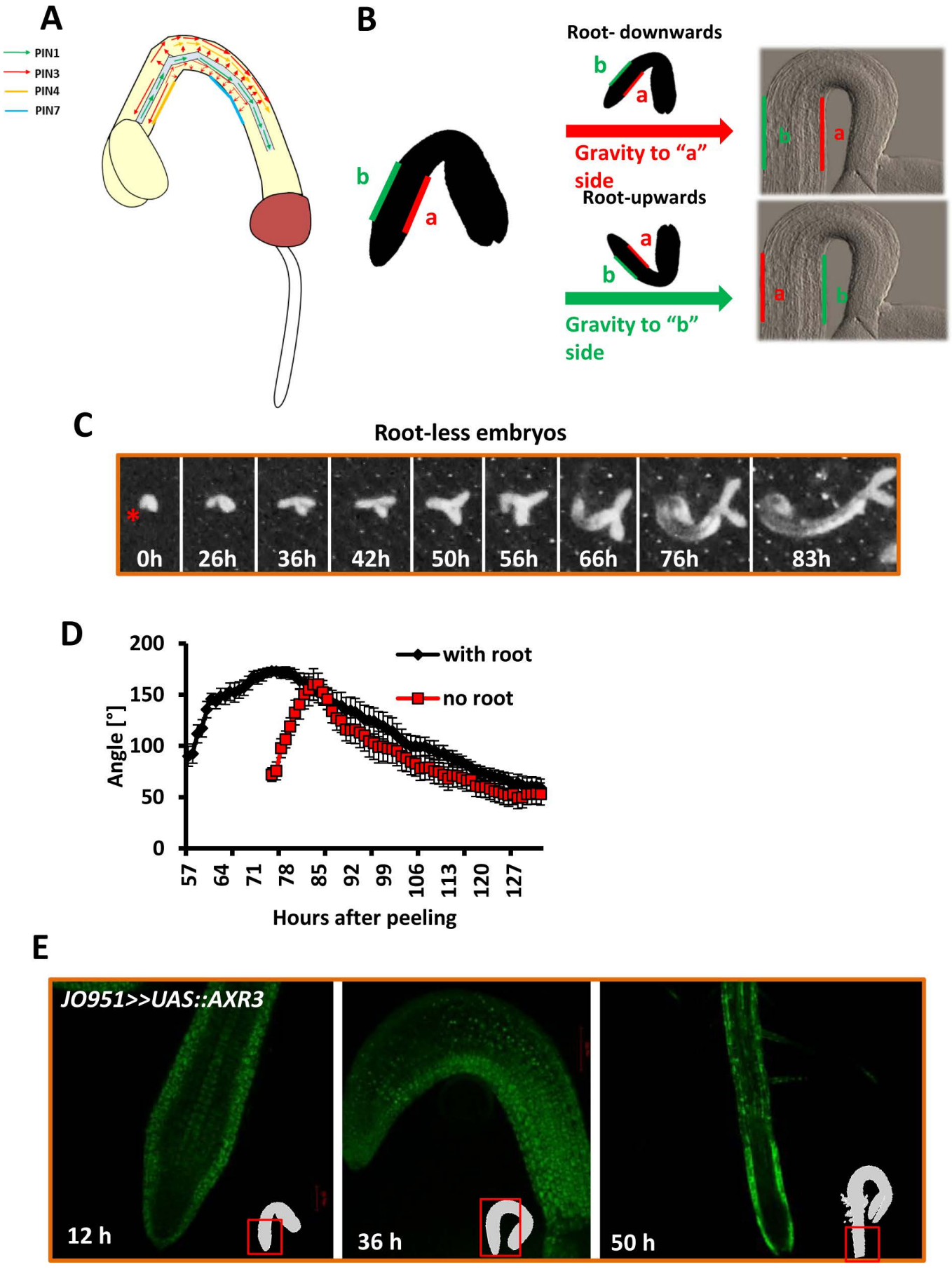

Figure S1. The root bending response to gravity guides the apical hook formation.

A. Model of auxin distribution during apical hook formation.

B. Scheme of mature embryos positioning to examine the impact of the embryonic shape on the apical hook formation. Mature embryos with the typical bent shape were dissected from seed coats and positioned on the media with root facing downwards or upwards. In the downwards and upwards orientation, either root side a or b, respectively, are gravity stimulated.

C-D. Real time monitoring of seedling growth after the embryonic root was detached. No apical hook formation could be detected (C). Kinetics of the apical hook development of intact and rootless seedlings (D). Red asterisk indicates the root pole position. Time in hours after transfer for incubation.

E. Expression analysis of J0951 activator using GFP reporter in roots of *J0951>>UAS::AXR3* seedlings. No GFP signal detected in roots at early phases of root growth (12 and 36h). 50h after start of incubation expression of GFP reporter at the root tip observed. Time in hours after transfer for incubation.

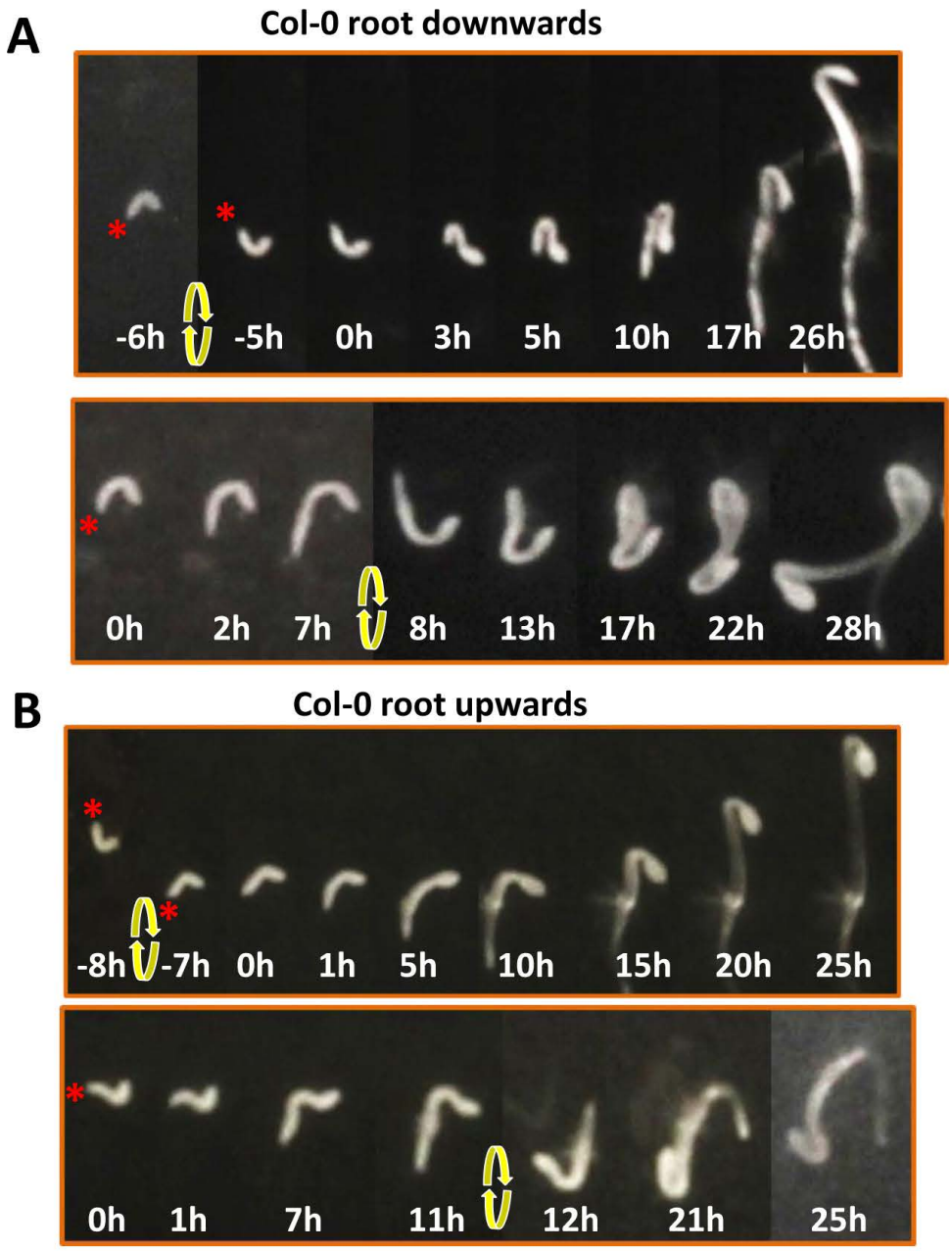

Figure S2. Root gravity driven bending coordinates the apical hook formation within a short developmental window.

A, B. Impact of changed gravity vector on the apical hook formation during germination of wild-type Col-0 seedlings. Seedlings positioned initially root down- (A) or upwards (B) were turned by 180 degrees at different time points. 0h indicates time of germination initiated by outgrowth of embryonic root and yellow arrows time of turning the plate. Red star indicates a root pole.

C,D. Real time monitoring of the apical hook formation in *scr-3* seedlings developing from mature embryos positioned in root downwards (A) and upwards (B) orientations. Time in hours after germination. Red star indicates a root pole.

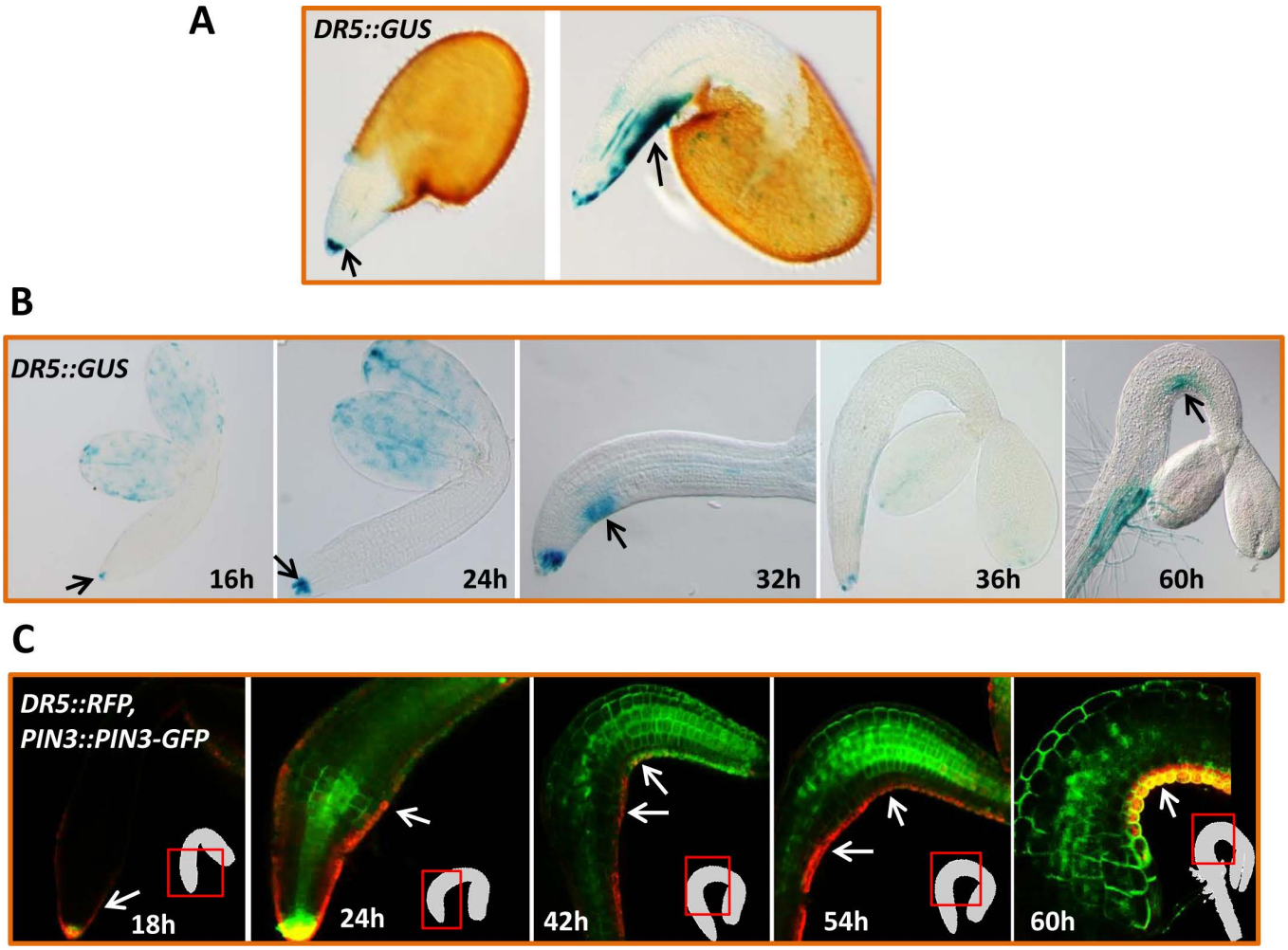

Figure S3. Monitoring of the auxin response during early phases of germination.

A. Auxin responses monitored using *DR5::GUS* reporter during early seed germination (radicle emergence). At first, auxin maximum detected in the root columella cells and afterwards at the gravi-stimulated side of the emerging root.

B. Monitoring of auxin responses during early phases of seedling development in darkness using *DR5::GUS* reporter. Auxin response maxima detected in the root columella (from 16h on). At 32h auxin response maximum observed at the root – hypocotyl junction, from 60h auxin response at the concave side of the apical hook detected.

C. Monitoring of the auxin response during early phases of seedlings developing in light using *DR5::RFP* reporter (red signal). Auxin maxima detected in the root columella (from 18h on). At 32h auxin response maximum detected at the root-hypocotyl junction, from 60h auxin response at the concave side of the apical hook detected. Green signal corresponds to *PIN3::PIN3-GFP* marker line. Time in hours after transfer for incubation (B,C.) Black (A, B) and white (C) arrows indicate the auxin response maximum.

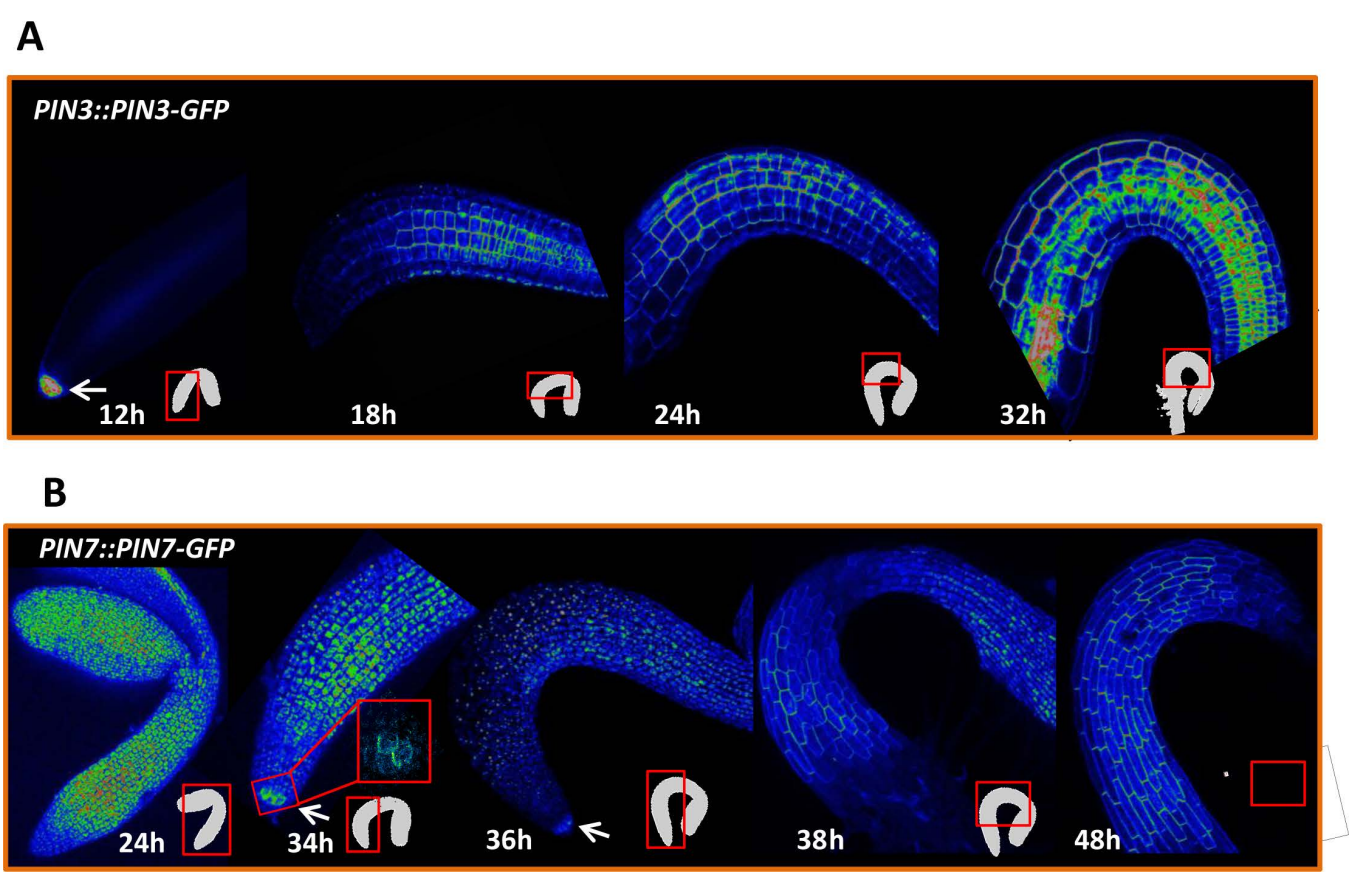

Figure S4. The expression pattern of PIN auxin efflux transporters during early phases of apical hook formation.

A. The earliest expression of *PIN3::PIN3-GFP* detected in the root columella cells at 12h after transfer for incubation. From 18h on PIN3-GFP detected in the hypocotyl, which progressively bends to form the apical hook.

B. Expression of *PIN7::PIN7-GFP* in the root columella detected 34h after transfer for incubation. PIN7-GFP in hypocotyl detected from 38h on.

White arrows indicate PIN-GFP signal in collumela. Insets indicate developmental stage of seedlings, red rectangle marks the zone magnified. Time in hours after transfer for incubation.

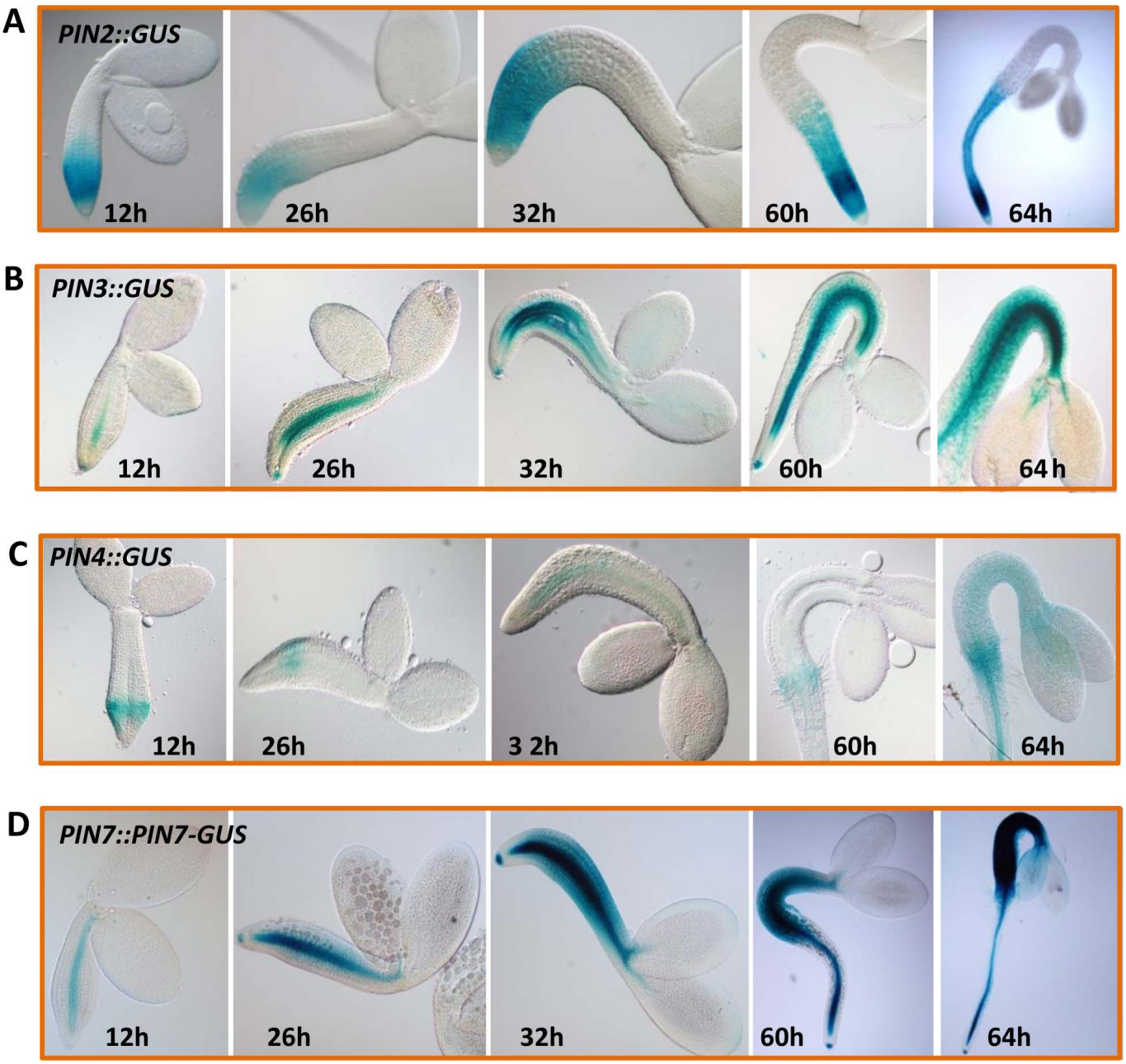

Figure S5. The pattern of *PINs* expression during early phases of the apical hook formation in darkness.

A-D. Monitoring of *PIN* genes (*PIN2::GUS* (A); *PIN3::GUS* (B); *PIN4::GUS* (C); and *PIN7::PIN7-GUS* (D)) expression during early phases of seedlings development. Time in hours after transfer for incubation.

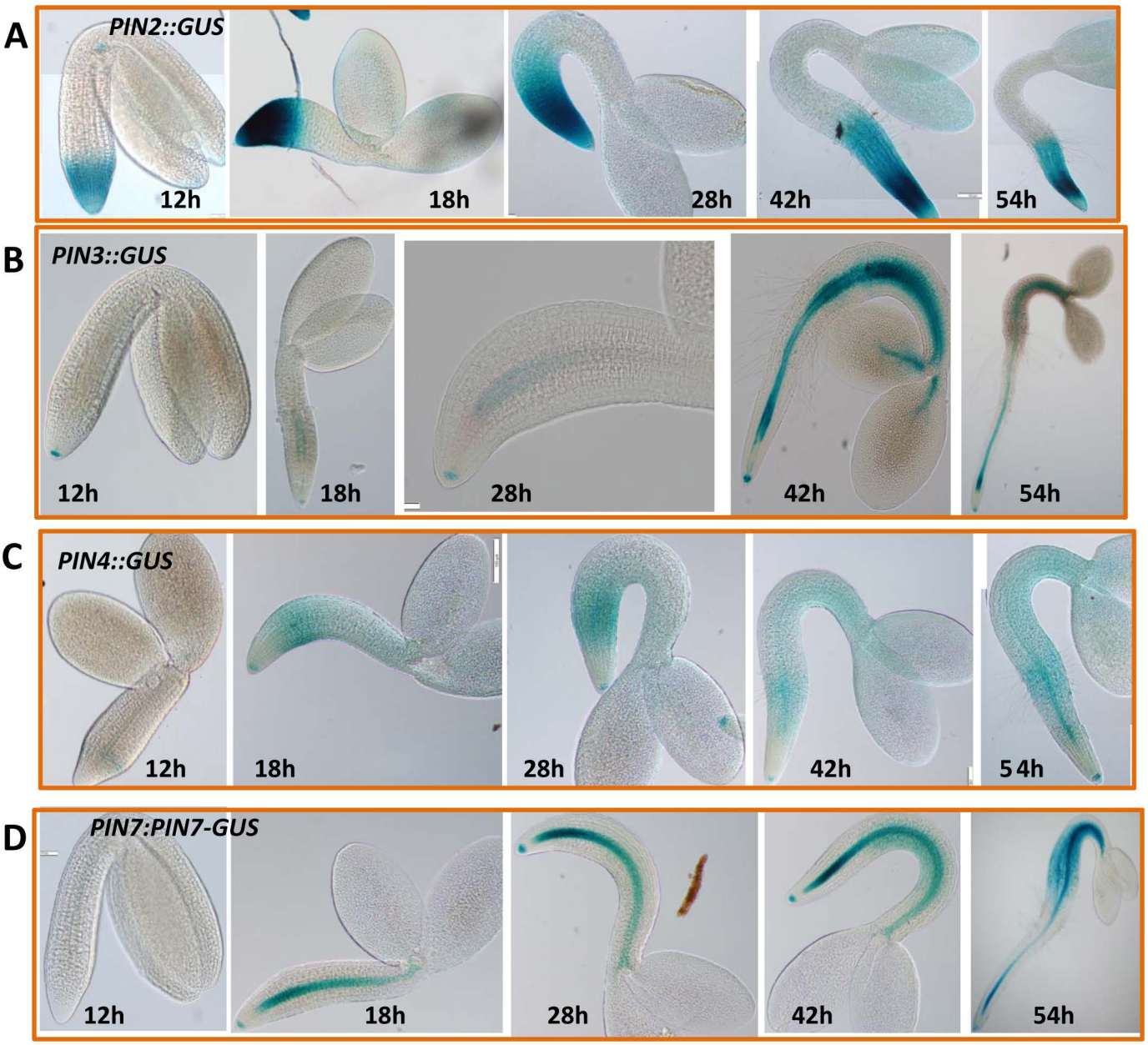

Figure S6. The pattern of *PINs* expression during early phases of the apical hook formation in light.

A-D. Monitoring of *PIN* genes (PIN2::GUS (A); *PIN3::GUS* (B); *PIN4::GUS* (C); and *PIN7::PIN7-GUS* (D)) expression during early phases of seedlings development. Time in hours after transfer for incubation.

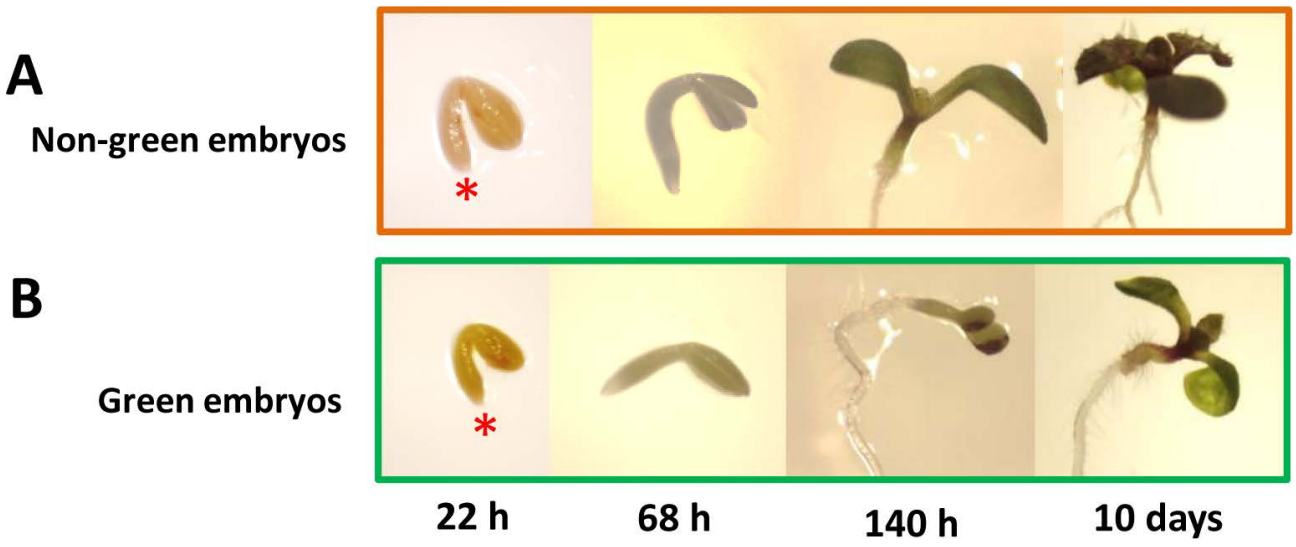

Figure S7. Seedlings developing from green embryos are viable.

A, B. Monitoring of seedlings developing from non-green (A) and green (B) mature embryo in the light. Red star indicates a root pole. Time in hours/days after transfer for incubation.

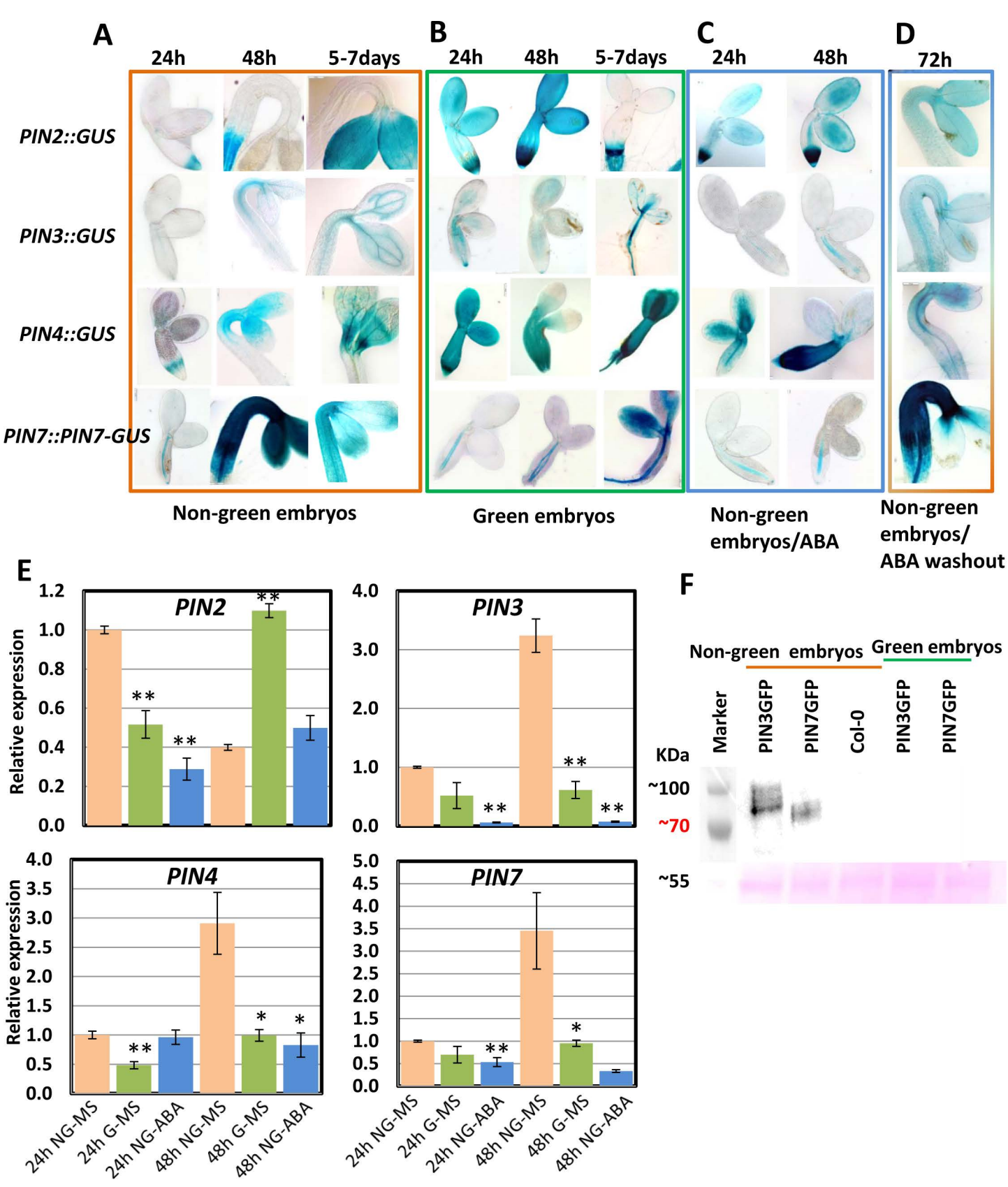

Figure S8. Monitoring of *PIN* expression in seedlings developing from green embryos and non-green embryos at presence of ABA.

A-D. Expression of *PIN:GUS* reporter lines in seedlings developing from non-green embryos (A), green embryos (B), non-green embryos at presence of 10µM ABA (C) and after ABA washout (D). Washout performed by growing seedlings for 48h on MS supplemented with 10µM ABA, followed by transfer of the seedlings back to MS media for 24h (D). Time in hours after start of incubation.

E. RT-qPCR analysis of PIN expression in seedlings developing from non-green embryos (NG, orange bar), green embryos (G, green bar) and non-green embryos treated with 10µM ABA (NG, blue bar). Time in hours after transfer for incubation. Asterisks indicate significant differences in transcript levels (Student t-test: *, $P < 0.05$; **, $P < 0.01$) between seedlings developing from green or non- green ABA treated Vs non-green embryos at the same time points. MS – Murashige and Skoog medium.

C. Analysis of PIN3-GFP and PIN7-GFP protein levels performed by Western-blot using GFP specific antibodies. Protein extracts obtained from seedlings of *PIN3:PIN3-GFP* and *PIN7:PIN7-GFP* lines developing from non- or green embryos for 72h in darkness. Expected size for PIN3-GFP is 95,5kDa and for PIN7-GFP is 93,6kDa. Ponceau staining of the membrane is shown as a loading control.

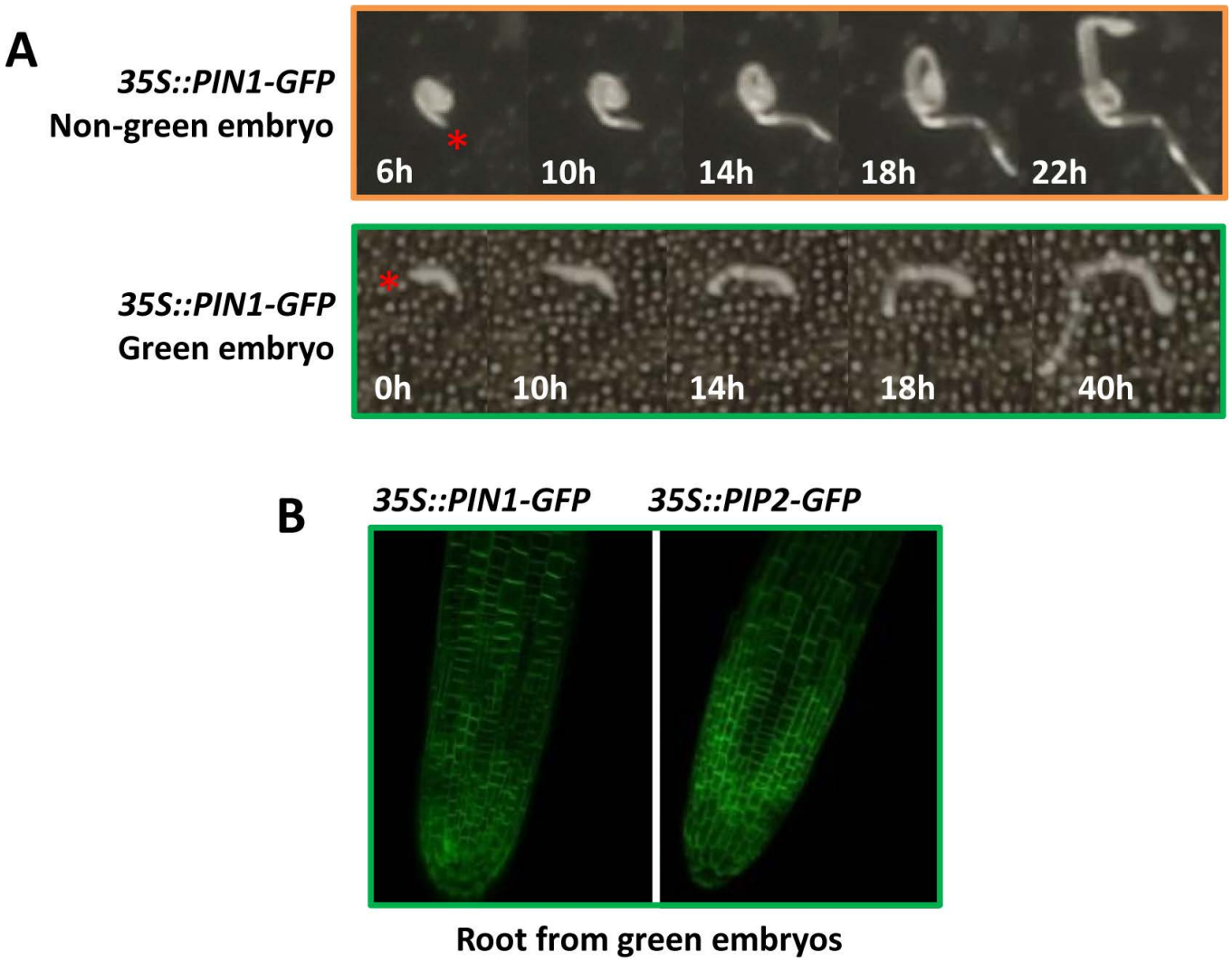

Figure S9. Ectopic expression of *PIN1* does not recover formation of the apical hook in seedlings developing from green embryos.

A. Real time monitoring of seedlings expressing PIN1-GFP under constitutive *35S* promoter, germinating from non- green and green embryos. Time in hours after germination.

B. PIN1 and PIP2 localizes to plasma membranes in root epidermal cells of *35S::PIN1-GFP* and *35S::PIP2-GFP* seedlings developing from green embryos.

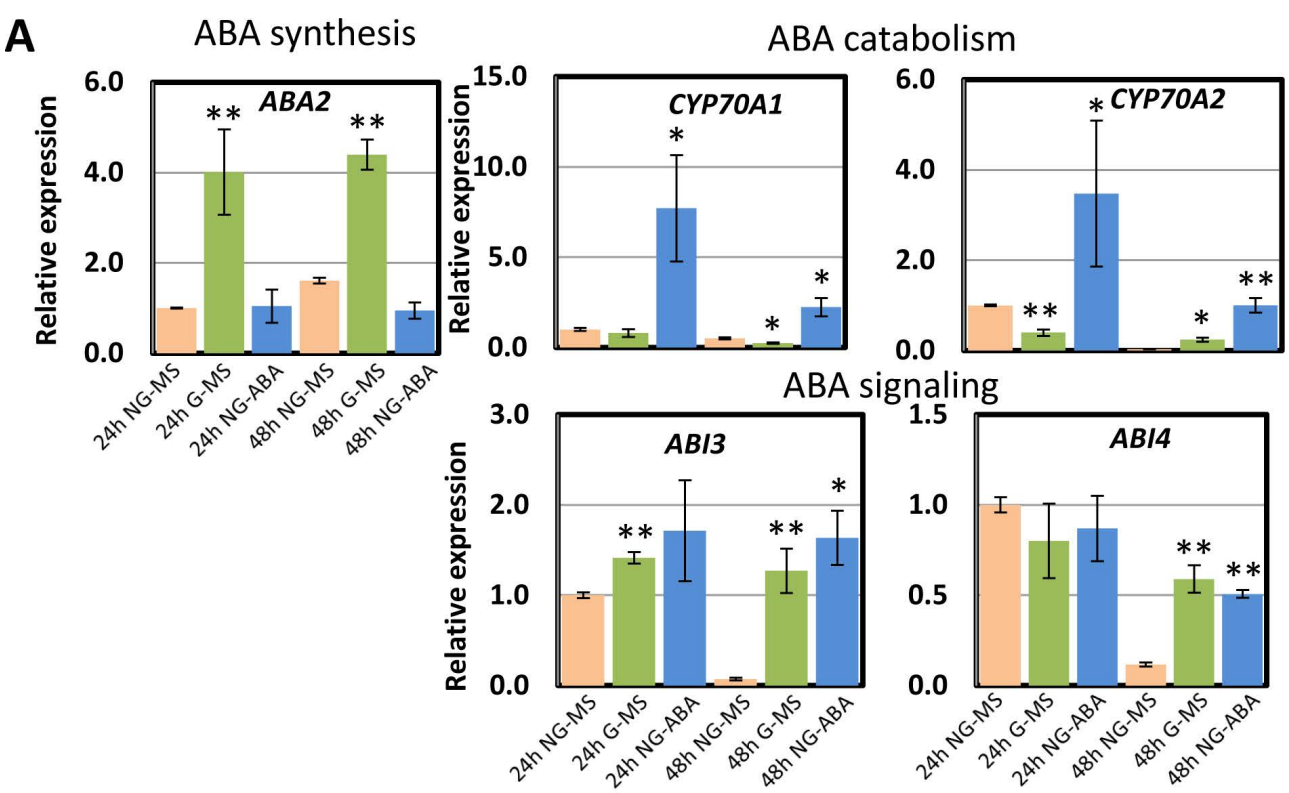

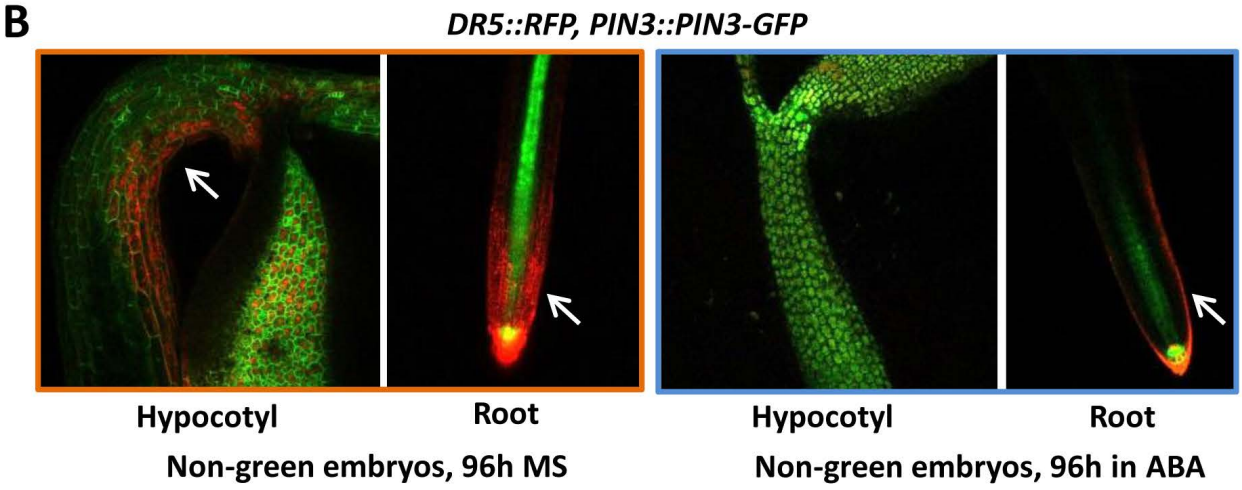

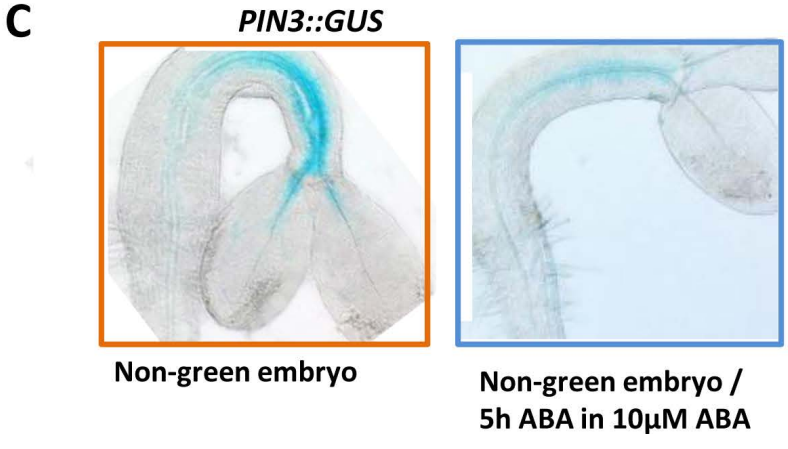

Figure S10. Development of seedlings from non-green embryos at presence of ABA mimics development of seedlings from green embryos.

A. Relative expression of ABA synthesis, catabolism and signaling genes during early stages of seedlings development from non-green embryos (NG, orange bar), green embryos (G, green bar) and non-green embryos treated with 10µM ABA (NG, blue bar). Time in hours after transfer for incubation. Asterisks indicate significant differences in transcript levels (Student t-test: *, $P < 0.05$; **, $P < 0.01$) between seedlings developing from green or non-green ABA treated Vs non-green embryos at the same time points. MS – Murashige and Skoog medium.

B. Monitoring of *DR5::RFP* auxin reporter expression during germination of seedlings from untreated and 0.1µM ABA treated non-green embryos. Reporter signal (red) is detected in the apical hook and at the root tip of untreated seedlings. In contrast, auxin maxima (red) observed in roots, but not hypocotyl of seedlings germinated from non-green embryos at presence of ABA. Green signal corresponds to *PIN3::PIN3-GFP* reporter. Time in hours after transfer for incubation. White arrows indicate auxin response maximum.

C. *PIN3::GUS* expression in seedlings treated with MS and MS supplemented with 10µM for 5 hours. MS – Murashige and Skoog medium. Experimental set up as for Figure 7B.

TABLE S1. Number of green embryos forming hook

Genotype	Col-0		
Treatment	**Seedlings wih hook**	**Seedlings without hook**	**% rescued**
AM	0	10	0.0
Abm	0	11	0.0
Abm+GA	0	12	0.0
	aba2-1		
Treatment	**Seedlings wih hook**	**Seedlings without hook**	**% rescued**
AM	0	22	0.0
Abm	1	21	**4.5**
Abm+GA	11	9	**55.0**
	Non-green embryos		
Treatment	**Seedlings wih hook**	**Seedlings without hook**	**% rescued**
AM	12	0	100.0
Abm	13	0	100.0
Abm+GA	9	0	100.0

Quantifications done from the experiment shown in Figure 8.

TABLE S2. Primers used for RT-qPCR

Name	Sequence	Gene\Seq
PIN2 F	TCACGACAACCTCGCTACTAAAGC	AT5G57090
PIN2 R	TGCCCATGTAAGGTGACTTTCCC	AT5G57090
PIN3 F	AAGGCGGAAGATCTGACCAAGG	AT1G70940
PIN3 R	TGCTGGATGAGCTACAGCTTTG	AT1G70940
PIN4 F	ACAACGTGGCAACGGAACAATC	AT2G01420
PIN4 R	GCCGATATCATCACCACCACTC	AT2G01420
PIN7 Fw	ATTGCGTGTGGCCATTGTTCAAGC	AT1G23080
PIN7 Rv	GCAACCACAAACGGCACGATCC	AT1G23080
ABI3 F	GGGAGGGACCTGGATGTATT	AT3G24650
ABI3 R	GCTCGGTCCATGGTAGGTAA	AT3G24650
ABI4 F	GTCCAGATGGGACAATTCCAACACC	AT2G40220
ABI4 R	CCCTAACGCCACCTCATGATGAAAC	AT2G40220
ABA2 F	TTCTCTTCCTAGTCAAAGGCTTT	AT1G52340
ABA2 R	GCAGACTTTGGCACCGTGCT	AT1G52340
CYP707A1-fw	TCATCTCACCACCAAGTA	AT4G19230
CYP707A1-rev	AAGGCAATTCTGTCATTCTA	AT4G19230
CYP707A2-Fw	ATCCATCACTCCTCCGAATTCTTCC	AT2G29090
CYP707A2-Rev	TCCATTTCCGAATGGCATGTACG	AT2G29090
PP2A F	TAACGTGGCCAAAATGATGC	AT1G69960
PP2A R	GTTCTCCACAACCGCTTGGT	AT1G69960

Movie 1. Apical hook development from embryos orientated in root-downwards position. Plasma membrane marker PIP2-GFP used to visualise plasma membranes.

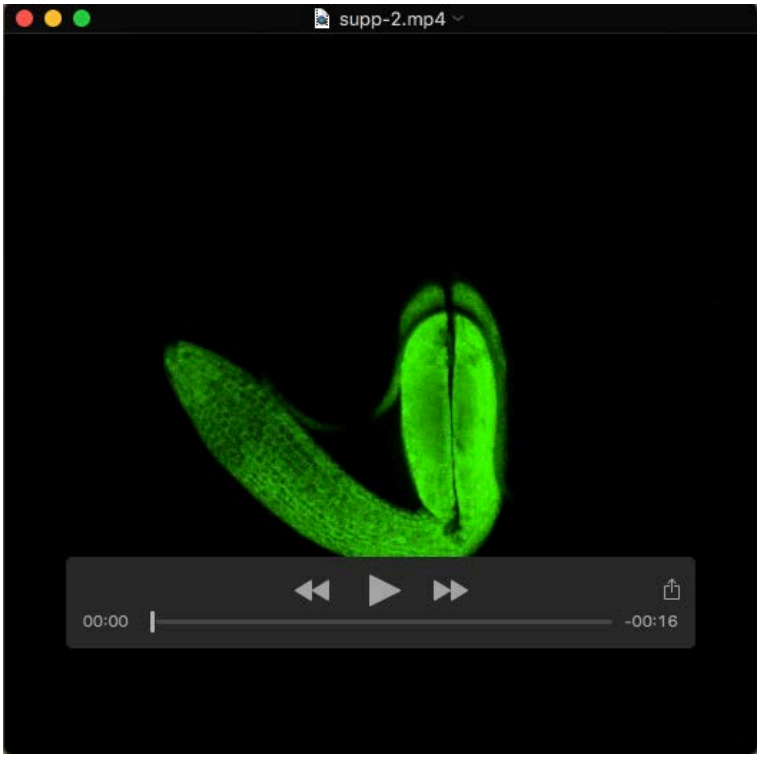

Movie 2. Apical hook development from embryos orientated in root- upwards position. Plasma membrane marker PIP2-GFP used to visualise plasma membranes.

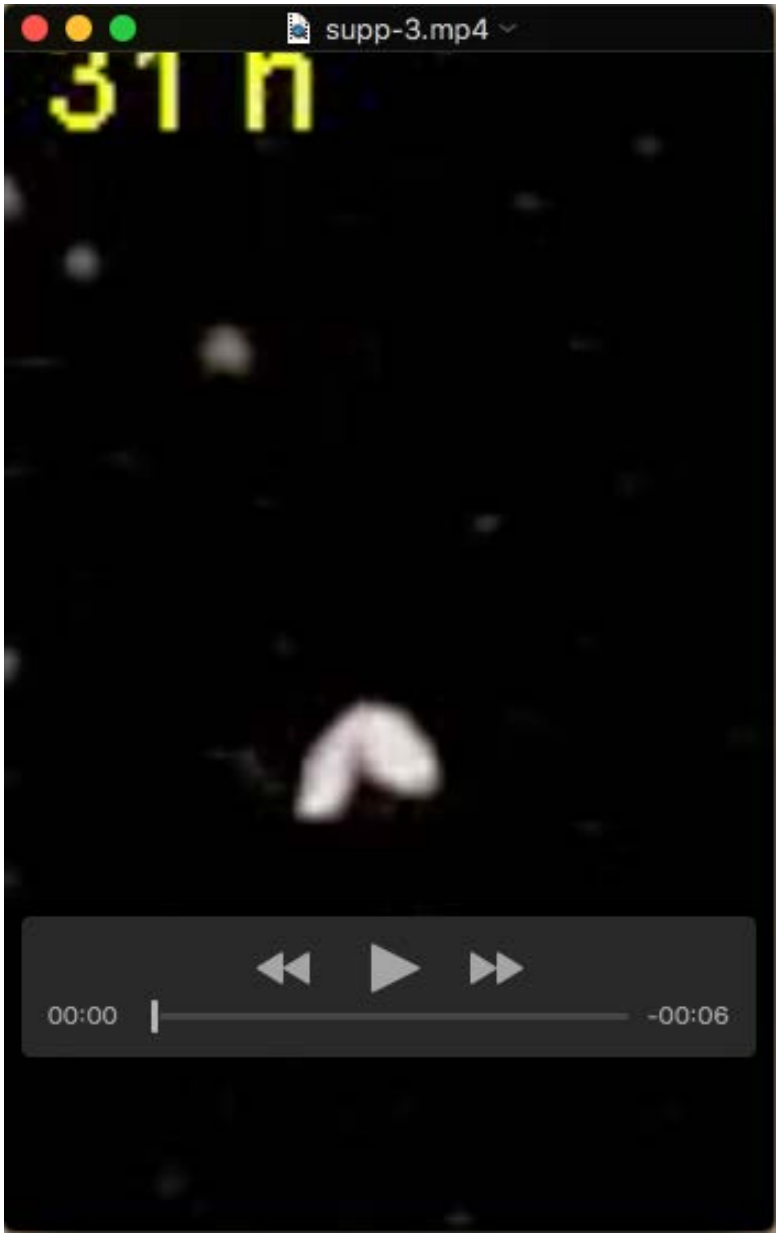

Movie 3. Apical hook development from embryos of *pin2* mutant orientated in root-downwards position.

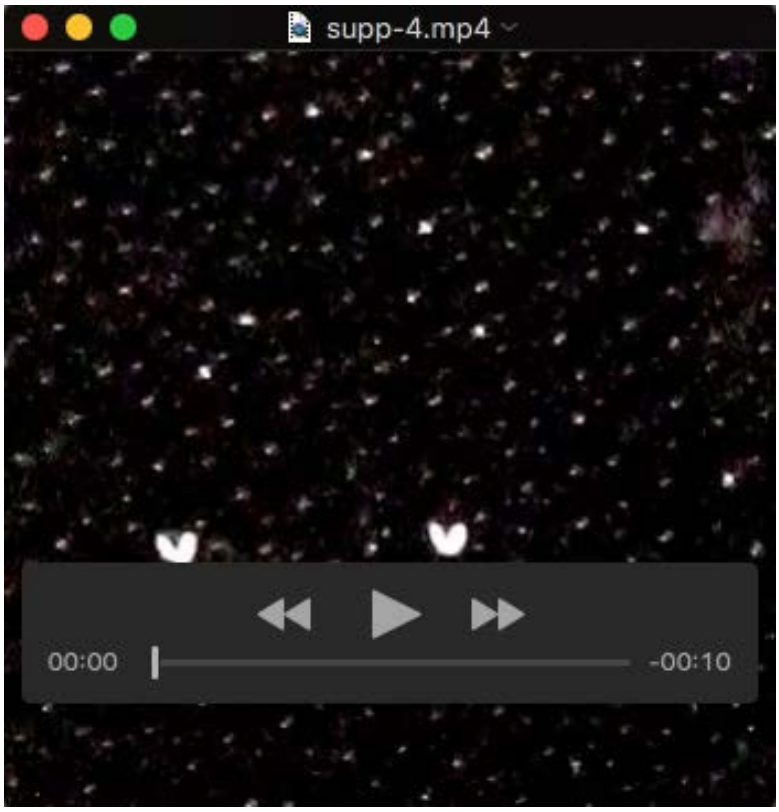

Movie 4. Apical hook development from embryos of *pin2* mutant orientated in root-upwards position.

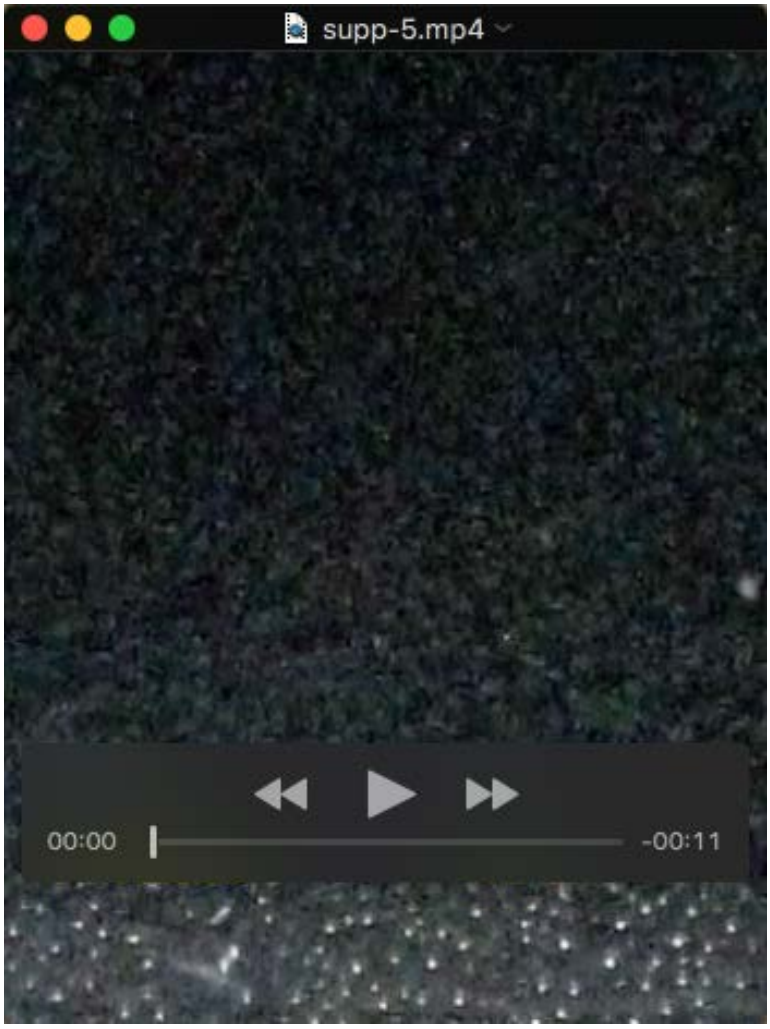

Movie 5. Apical hook development in *rml* mutant and Col-0 control.

Movie 6. Apical hook development from embryos of F1 progeny of *J0951>>UAS::AXR3*, orientated in root-downwards position.

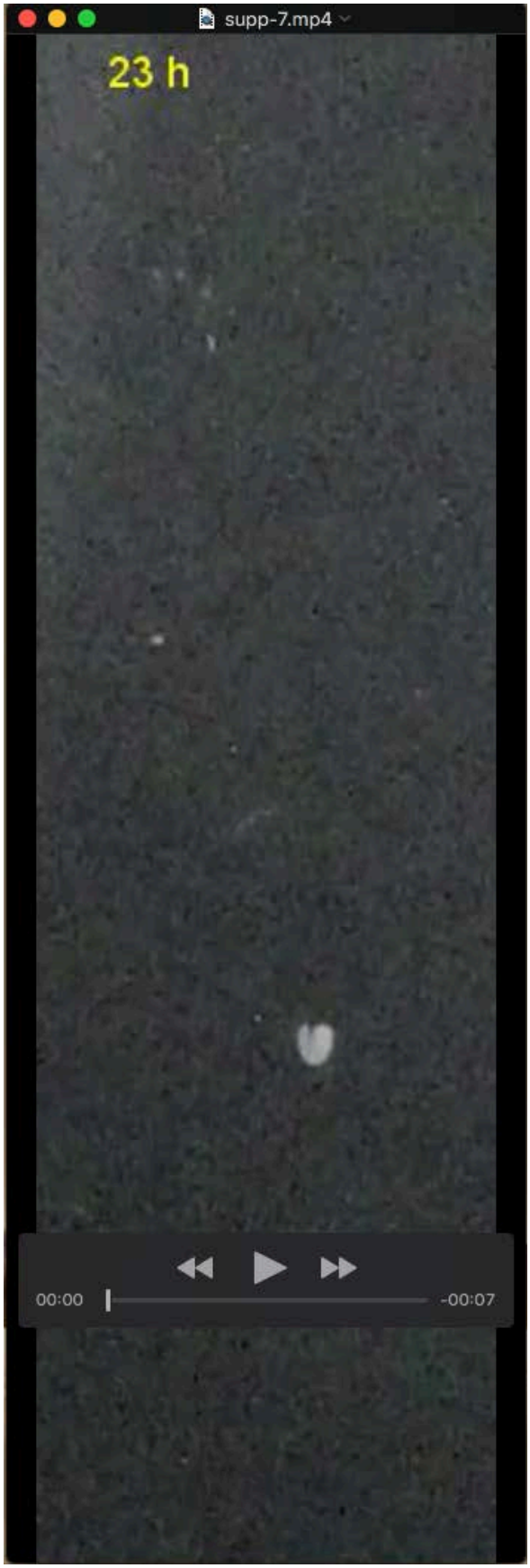

Movie 7. Apical hook development from embryos of F1 progeny of *J0951>>UAS::AXR3*, orientated in root- upwards position.

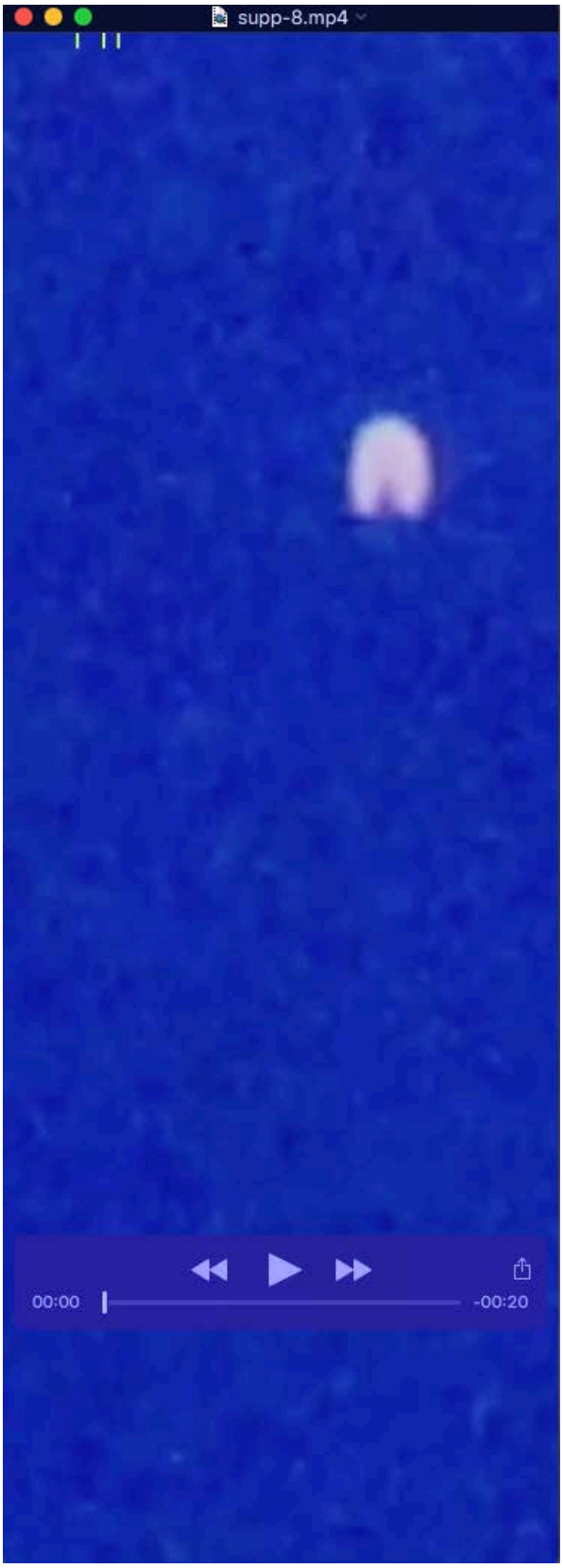

Movie 8. Apical hook development from embryos of Col-0 orientated in root-downwards position under constant light.

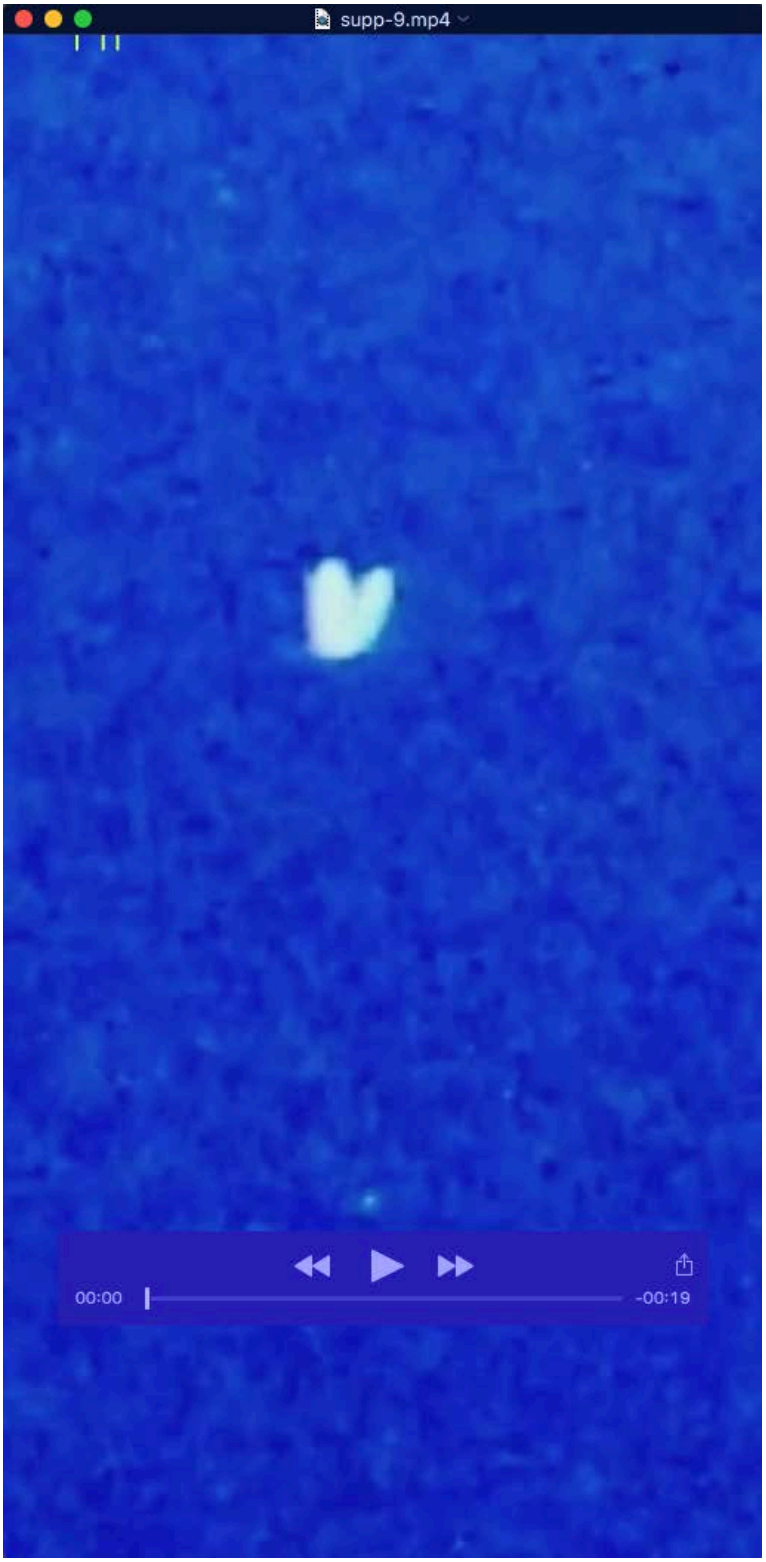

Movie 9. Apical hook development from embryos of Col-0 orientated in root- upwards position under constant light.

Movie 10. Germination of seedlings from green embryos orientated in root-downwards position, in darkness.

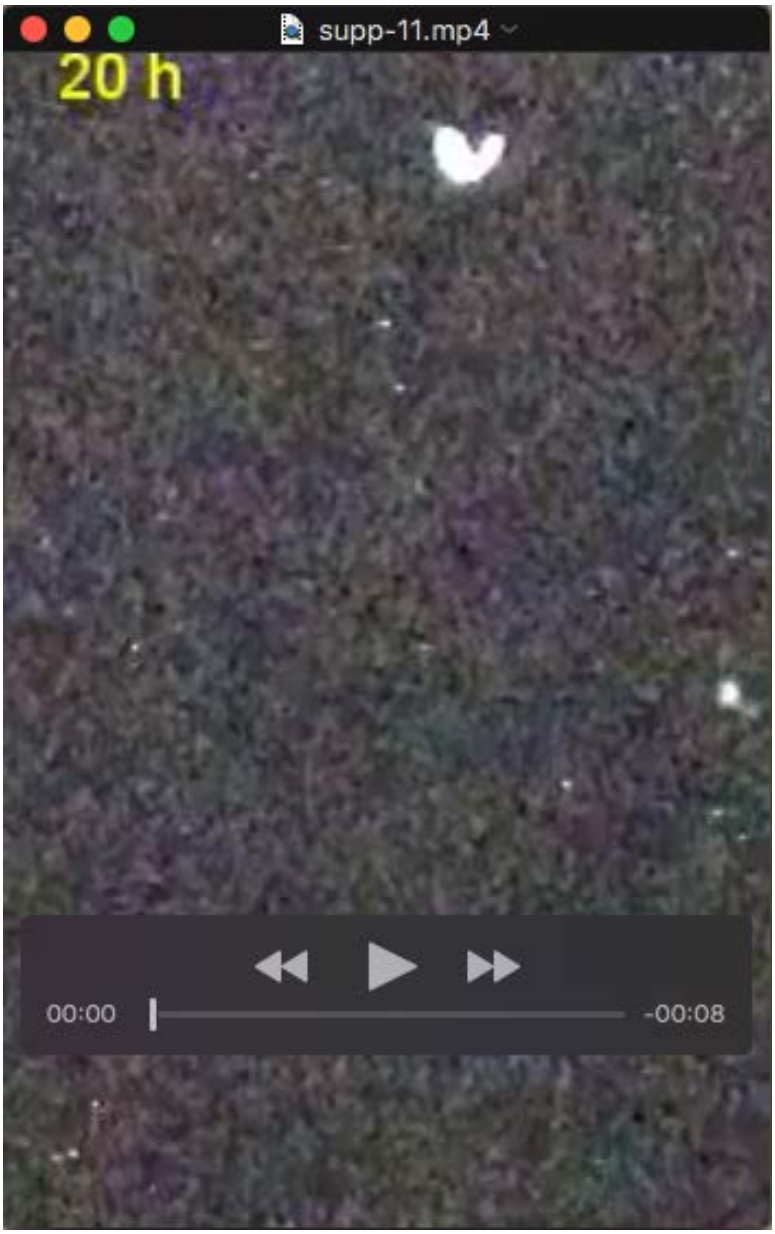

Movie 11. Germination of seedlings from green embryos orientated in root-upwards position, in darkness.